

APPLICATION OF THE METHOD OF INTEGRAL-RELATIONS
TO SUPERSONIC AND HYPERSONIC FLOW
PAST PARABOLOIDS OF REVOLUTION

BY

Ming-Yang Su

Thesis submitted to the Graduate Faculty of the
Virginia Polytechnic Institute
in candidacy for the degree of
MASTER OF SCIENCE
in
Aerospace Engineering

August 1964

Blacksburg, Virginia

TABLE OF CONTENTS

Chapter	Page
I. LIST OF FIGURES	4
II. INTRODUCTION.....	5
III. LIST OF SYMBOLS	12
(A) Non-dimensionalizing Quantities	12
(B) General Symbols	12
IV. DERIVATIONS OF GOVERNING EQUATIONS	15
(A) Non-dimensionalizing the Variables ...	15
(B) Governing Equations in Orthogonal Curvilinear Coordinates	16
(C) Transforming into Divergence Form	19
(D) Oblique Shock Relations	23
(E) Applying the First Approximation	27
(F) Geometry of the Paraboloid of Revolution	31
(G) Boundary Conditions and the Methods of Solving the Differential Equations ...	33
V. METHODS AND DISCUSSION OF COMPUTER CALCULATION	36
VI. DISCUSSION OF CALCULATED RESULTS	39

TABLE OF CONTENTS (Continued)

Chapter	Page
VII. CONCLUSIONS	42
VIII. SUMMARY	43
IX. ACKNOWLEDGEMENTS	44
X. BIBLIOGRAPHY	45
XI. VITA	48

I. LIST OF FIGURES

	Page
Figure 1. Coordinate System and Associated Quantities	49
Figure 2. Variation of Stagnation Shock Detachment Distance with Mach Number ..	50
Figure 3. Variation of Δ with u_0 for various δ_{sp} at $M_\infty = 3$	51
Figure 4. Shock Shapes and Sonic Lines for $\gamma = 1.4$	52
Figure 5. Shock Shapes and Sonic Lines for $\gamma = 5/3$	53
Figure 6. Velocity Variation along the Body Surface for $\gamma = 1.4$	54
Figure 7. Velocity Variation along the Body Surface for $\gamma = 5/3$	55
Figure 8. Pressure Distribution on the Body Surface for $\gamma = 1.4$	56
Figure 9. Pressure Distribution on the Body Surface for $\gamma = 5/3$	57

II. INTRODUCTION

The importance of the blunt-body problem in aerodynamics can be appreciated from the fact that at high flight speeds even slender bodies must incorporate some nose bluntness to provide sufficient surface area for reduction of heat-transfer rates in the nose stagnation region. Also, theory predicts that the body with a blunted nose, not the sharp-nosed body, will give minimum drag at hypersonic speeds.

Supersonic flow past a blunt body produces a detached, bow shock wave with a restricted region of subsonic flow between the shock wave and that part of the body in the vicinity of the stagnation point. This generally results in a supersonic flow for the remainder of the flow field downstream of this subsonic region. For any body meridian plane, parallel to the freestream direction, the supersonic flow behind the shock wave is "separated" from the subsonic region by an imaginary sonic line which joins a point on the shock profile to a point on the body. Everywhere along this line the local Mach number is unity. Mathematically, the governing differential equation for the subsonic region is an elliptic type, while that for the supersonic region is hyperbolic. For a completely supersonic flow there are known exact methods of solution; for instance, the method of characteristics. However, for the mixed subsonic-supersonic

flow region, there exists a difficult and different type of problem. Many investigations on this subject have been carried out (since 1945), utilizing various analytical methods. Freeman (Ref. 8) and Chester (Ref. 5) have employed the so-called "thin shock layer theories", which assumes the region between the bow shock wave and the body (i.e., the shock layer) to be small compared with other flow properties.

Cabannes (Ref. 11) attacked the problem by expanding certain flow quantities in a Taylor series (from the shock wave), while Lighthill (Ref. 11) used a constant-density analysis.

Desirable as they are, these analytical approaches usually give either very rough results from the practical point of view, or are applicable only to a very narrow region near ~~to~~ the stagnation point.

In order to obtain more accurate results for design purposes, numerical methods are needed. Here again one may take two essentially different approaches; one which is "direct", and the other "inverse". In the direct method the shape of the body is given. One then determines the shape of the shock wave, the flow variables in the shock layer, and the pressure distribution on the body. In the inverse method a shock shape is assumed, and it is then required to find the corresponding body shape and the flow details

within the shock layer.

It is apparent that the direct method is more significant and desirable than the inverse scheme since in a practical case one generally is required to find the flow field (including the shock shape) produced by a given body shape.

Among the several existing direct methods there are streamtube-continuity methods, relaxation techniques, and the method of integral relations.

Two schemes using the first method have been devised, one by Maslen and Moeckel (Ref. 15) and the other by Uchida and Yasuhara (Ref. 22). The method of Maslen and Moeckel, although simple to apply since it requires iteration of only the shock shape, is nevertheless a very rough approximation. In addition, it requires -- as a starting point of the calculations -- a knowledge of the surface pressure distribution, which is unknown a priori. On the other hand, the method of Uchida and Yasuhara is exact in principle, yet very laborious, since it requires an iteration for the shock shape and the streamline pattern. Too, this method possesses the disadvantage of being somewhat difficult to program for electronic computations.

The second direct approach is the relaxation method of Southwell, which has been employed by Maccoll and Codd (Ref. 14) and Mitchell (Ref. 16). Although this technique is

applicable to the problem at hand, it too has the disadvantage of being laborious and generally ill suited for electronic computer usage.

The need for numerical schemes suitable for machine computation cannot be over emphasized. As flight speeds continue to increase, various additional effects, associated with a strong bow shock wave and very high temperatures, such as dissociation, ionization, radiation, electronic excitation, and so forth, become more and more significant. It then follows that the governing differential equations become even more complicated. Consequently, doubts arise as to whether it would be possible to construct adequate experimental equipment capable of simulating model tests under these extreme conditions. It seems quite possible that in the future, aerodynamic experiments will give only basic physical relations and constants, while the gas flow characteristics will have to be calculated. If such conditions do arise, then the electronic computer will prove to be even more indispensable than it is at present.

In 1957 Dorodnitsyn (Ref. 7) proposed a general method of integral-relations for nonlinear fluid dynamics problems. Although quite lengthy, this numerical scheme does have the important advantage of being suited to automatic digital computation and is applicable to the mixed flow problem of subsonic-supersonic flow. This method was first used by

Belotserkovskii (Ref. 2) to calculate the supersonic flow past a circular cylinder. Subsequently it was employed by Chuskin (Ref. 6) to calculate the transonic flow past ellipsoids. Later, Gold and Holt (Ref. 9) extended Belotserkovskii's method to deal with the supersonic flow past a flat-headed circular cylinder; and Traugott (Ref. 19) applied the same method to supersonic blunt-body problems for arbitrary axisymmetric shapes. Lately Jerry South, Jr. (Ref. 18) has applied this method to nonequilibrium flow over pointed bodies.

The method of integral-relations consists of dividing the shock layer into one, two, or more strips, which are parallel to the body surface, depending on the accuracy desired. The more the number of strips, the more accurate the result will be. The calculation using N strips will be denoted as ^{the} N th approximation.

The coordinate system employed is taken with reference to the body. That is, one coordinate is measured along the body surface, with the second coordinate measured normal to the body locally. The governing nonlinear partial differential equations are then integrated outward from the body surface to the boundary of each strip. This is accomplished by assuming that the physical variables within these strips can be expressed by appropriate interpolation formulas. In this fashion the equations are reduced to a finite system of

simultaneous first-order, nonlinear, ordinary differential equations. These can be solved numerically as a two-point boundary value problem, starting at the stagnation point and passing through a critical region near the sonic point on the body. Since we are studying only $\frac{d\eta}{dx}$ axisymmetric flow field, the nose of the body under consideration must be a stagnation point. Thus the boundary conditions at the nose can be readily determined. The other boundary condition at the sonic point on the body is more involved and will be discussed in later sections where it is needed.

Belotserkovskii calculated the supersonic flow past circular cylinders (Ref. 2) employing first, second, and third approximations, consecutively (that is, he divided the shock layer into one, two, and three strips, respectively); the results using the first approximation are good, but those using the second approximation give better agreement with experiments; and the third approximation gives essentially the same numerical results as the second approximation. Chuskin carried out the calculation for the transonic flow past an ellipsoid (Ref. 6) using the second and third approximations. All the other investigators thus far have used the first approximation only. The total number of equations resulting from the integrations across all strips will be $(4N-1)$ for the N th approximation. Of this number, $3N$ are ordinary differential equations, while the remaining

(N-1) equations are algebraic relations. Thus the work needed for approximations greater than the first is tremendous.

In this thesis, the first approximation of the integral-relations method is used to investigate supersonic and hypersonic flow past paraboloids of revolution. The shock shape, location of sonic line, and the pressure distribution on the bodies are calculated at freestream Mach numbers of 3, 4, 6, 10, and 1000 (taken as infinite) for two different values of the ratio of specific heats; namely $\gamma = 5/3$ and $\gamma = 1.4$. The first case (for γ) corresponds to an ideal monoatomic gas while the second one corresponds to ideal diatomic gases.

Unfortunately, no experimental data have been found in the literature for supersonic flows past this particular body shape. Therefore, the calculated results are compared with those obtained by Van Dyke's inverse method (Ref. 24).

III. LIST OF SYMBOLS

(A) Non-dimensionalizing Quantities

1. Pressure:

p_0' = freestream stagnation value

2. Density:

ρ_0' = freestream stagnation value

3. Velocity:

$$V'_{\max} = \sqrt{\frac{2\gamma}{\gamma-1} \left(\frac{p_0'}{\rho_0'}\right)}$$

4. Distance:

R'_{sp} = body nose radius of curvature

(B) General Symbols*

a = speed of sound

$$g = \rho u^2 + \left(\frac{\gamma-1}{2\gamma}\right) p$$

$$h = v(1 - w^2)^{\frac{1}{\gamma-1}}$$

$$H = \rho v^2 + \left(\frac{\gamma-1}{2\gamma}\right) p$$

*General symbols appearing in the thesis development with a superscripted prime attached to them are meant to be dimensional.

Unprimed symbols appearing for pressure, density, velocity, and distance indicate quantities which have been made non-dimensional by dividing by the appropriate non-dimensionalizing term p_0' , ρ_0' , V'_{\max} , or R'_{sp} .

M = Mach number

n = distance normal to the body surface

p = pressure

r = radial distance normal to the body axis

R = radius of curvature of the body contour

S = entropy

s = distance along the body surface measured from the
stagnation point

$$t = u(1 - w^2)^{\frac{1}{\gamma-1}}$$

u = velocity component parallel to the body surface

v = velocity component normal to the body surface

$$w = \sqrt{u^2 + v^2} = \text{total local speed}$$

X = axial distance measured from the stagnation point

x = angle between a normal to the axis of symmetry and
the tangent to the shock wave

z = ρuv

δ = shock layer thickness measured from and normal to
the body surface

ρ = density of the fluid

θ = angle between the axis of symmetry and the local
body surface tangent

$$\phi = p/\rho^\gamma$$

γ = specific heat ratio

τ = dimensionless time defined as time divided by
 (R'_{sp} / V'_{max})

Subscript

- ∞ refers to freestream conditions
- 0 refers to conditions on the body surface
- 1 refers to conditions just behind the shock
- sp refers to conditions at the stagnation point

III. DERIVATION OF GOVERNING EQUATIONS

Consider the supersonic (and hypersonic) flow of a perfect gas with constant specific heats past a paraboloid of revolution. Far upstream of the body the flow is uniform, whereas a detached shock wave forms immediately ahead of the body. The shape and position of the shock is unknown beforehand; actually this is what must be determined, at a given Mach number and a specified ratio of specific heats. One introduces non-dimensional variables and certain other quantities (in order to transform the governing equations into the divergence form), which is what is needed to apply the method of integral-relations.

Afterward, the shock relations and the conditions on the body surface are derived, then the governing equations can be integrated across the shock layer. In this manner one is able to reduce the problem to three ordinary differential equations, which can be solved by numerical schemes.

(A) Non-dimensionalizing the Variables

In order to facilitate the non-dimensionalization we shall take the radius of curvature of the nose of the body, (R'_{sp}), the stagnation density in the freestream, (ρ'_0), the stagnation pressure in the freestream, (p'_0), and the maximum

speed in the freestream, $(V'_{\max} = \sqrt{(\frac{2\gamma}{\gamma-1}) \frac{p_0}{\rho_0}})$, as the characteristic length, density, pressure, and speed, respectively. The non-dimensional quantities are then defined as follows:

$$\begin{aligned} s &= \frac{s'}{R'_{sp}} \quad , \quad n = \frac{n'}{R'_{sp}} \quad , \quad R = \frac{R'}{R'_{sp}} \quad , \\ v &= \frac{v'}{V'_{\max}} \quad , \quad u = \frac{u'}{V'_{\max}} \quad , \quad a = \frac{a'}{V'_{\max}} \quad , \quad (A-1) \\ p &= \frac{p'}{p_0} \quad , \quad \rho = \frac{\rho'}{\rho_0} \quad \text{and} \quad w = \sqrt{u^2 + v^2} \quad . \end{aligned}$$

where the local radius of curvature of the body surface in the meridian plane is given by

$$R = \frac{1}{-(\frac{d\theta}{ds})} = -\frac{ds}{d\theta} \quad . \quad (A-2)$$

(R will be positive where the body is convex outward.) In addition to the above, the following non-dimensional quantities are also defined:

$$t = u(1 - w^2)^{\frac{1}{\gamma-1}} \quad (A-3-a)$$

$$h = v(1 - w^2)^{\frac{1}{\gamma-1}} \quad (A-3-b)$$

$$z = \rho uv \quad (A-3-c)$$

$$H = \rho v^2 + \left(\frac{\gamma-1}{2\gamma}\right) p \quad (A-3-d)$$

and

$$g = \rho u^2 + \left(\frac{\gamma-1}{2\gamma}\right) p \quad . \quad (A-3-e)$$

These quantities are to be used in transforming the governing equations into the divergence form.

(B) Governing Equations in Orthogonal Curvilinear Coordinates

Consider a steady, invicid, compressible and rotational fluid flow. The non-dimensional momentum equation for the flow field can be expressed in vector form as

$$\nabla \left(\frac{\bar{w}^2}{2} \right) - \bar{w} \times (\nabla \times \bar{w}) + \left(\frac{\gamma-1}{2\gamma} \right) \frac{1}{\rho} \nabla p = 0 \quad . \quad (B-1)$$

Referring to Fig. 1, and using the orthogonal curvilinear coordinates (s,n) for an axisymmetric flow, it can be shown that the scale factors (in s- and n-directions) are, respectively,

$$h_s = 1 + \frac{n}{R} \quad \text{and} \quad h_n = 1 \quad .$$

In terms of these coordinates the velocity is

$$\bar{w} = u \bar{e}_s + v \bar{e}_n \quad .$$

The ∇ operator then can be expressed by

$$\nabla = \frac{1}{\left(1 + \frac{n}{R}\right)} \bar{e}_s \frac{\partial}{\partial s} + \bar{e}_n \frac{\partial}{\partial n} \quad . \quad (B-2)$$

Using this operator, Eq. (B-1) can be converted into two components, giving the s-direction momentum equation as

$$u \frac{\partial u}{\partial s} + \left(1 + \frac{n}{R}\right) v \frac{\partial u}{\partial n} + \frac{uv}{R} + \left(\frac{\gamma-1}{2\gamma}\right) \frac{1}{\rho} \frac{\partial p}{\partial s} = 0 \quad , \quad (B-3)$$

and the n-direction momentum equation as

$$u \frac{\partial v}{\partial s} + \left(1 + \frac{n}{R}\right) v \frac{\partial v}{\partial n} - \frac{u^2}{k} + \left(\frac{\gamma-1}{2\gamma}\right) \frac{1}{\rho} \left(1 + \frac{n}{R}\right) \frac{\partial p}{\partial n} = 0 \quad . \quad (B-4)$$

The continuity equation is known to be

$$\bar{\nabla} \cdot (\rho \bar{w}) = 0$$

or, expanding, it is

$$\frac{\partial}{\partial s} (\rho u) + \frac{\partial}{\partial n} \left[\left(1 + \frac{n}{R}\right) \rho v \right] = 0 \quad . \quad (B-5)$$

Now, in place of the s-momentum equation one can introduce the Bernoulli equation for steady compressible flow; that is

$$\frac{w'^2}{2} + \left(\frac{\gamma}{\gamma-1}\right) \frac{p'}{\rho'} = \left(\frac{\gamma}{\gamma-1}\right) \frac{p_0'}{\rho_0'} \quad (B-6)$$

and using Eq. (A-1), Eq. (B-6) can be rewritten as

$$\frac{p}{\rho} = 1 - w^2 \quad . \quad (B-7)$$

In terms of pressure and density, the entropy, (S), can be expressed by

$$S = c_v \ln\left(\frac{p}{\rho^\gamma}\right) + \text{constant} \quad (B-8)$$

where c_v is the specific heat at constant volume.

Next, taking the substantive derivative of S,

$$\frac{DS}{Dt} = 0 = c_v \frac{D}{Dt} \left[\ln\left(\frac{p}{\rho^\gamma}\right) \right] = c_v \frac{\rho^\gamma}{p} \frac{D}{Dt} \left(\frac{p}{\rho^\gamma}\right) \quad ,$$

since entropy remains constant along a streamline, then

$$\frac{D}{Dt} \left(\frac{p}{\rho^\gamma} \right) = 0 \quad .$$

The integration of the equation gives

$$\frac{p}{\rho^\gamma} = \phi \quad , \quad (B-9)$$

where ϕ is an arbitrary function dependent upon the stream function.

Using Eqs. (B-7) and (B-9), the pressure and density can next be expressed as

$$p = (1 - w^2)^{\frac{\gamma}{\gamma-1}} \phi^{-\frac{1}{\gamma-1}} \quad (B-10)$$

and

$$\rho = (1 - w^2)^{\frac{1}{\gamma-1}} \phi^{-\frac{1}{\gamma-1}} \quad (B-11)$$

respectively.

(C) Transforming into Divergence Form

In this section the governing equations derived previously will be transformed into divergence form.

Using Eq. (B-11), then from Eqs. (A-3-a) and (A-3-b)

$$t \equiv u(1 - w^2)^{\frac{1}{\gamma-1}} = \rho u \phi^{\frac{1}{\gamma-1}} \quad (C-1)$$

and

$$h \equiv u(1 - w^2)^{\frac{1}{\gamma-1}} = \rho v \phi^{\frac{1}{\gamma-1}} \quad . \quad (C-2)$$

Substituting Eqs. (C-1) and (C-2) into Eq. (B-5), the continuity equation becomes

$$\frac{\partial}{\partial s} (rt) + \frac{\partial}{\partial n} \left[\left(1 + \frac{n}{R}\right) rh \right] = 0 \quad . \quad (C-3)$$

Multiplying Eq. (B-4) by ρr and Eq. (B-5) by v , then after adding and rearranging, one obtains

$$\begin{aligned} \frac{\partial}{\partial s} (\rho r u v) + \frac{\partial}{\partial n} \left[\left(1 + \frac{n}{R}\right) \rho r v^2 \right] + \rho r R u^2 \\ + \left(\frac{\gamma-1}{2\gamma}\right) \frac{\partial}{\partial n} \left[\left(1 + \frac{n}{R}\right) r p \right] - \left(\frac{\gamma-1}{2\gamma}\right) r p \frac{\partial}{\partial n} \left(1 + \frac{n}{R}\right) \\ - \left(\frac{\gamma-1}{2\gamma}\right) \left(1 + \frac{n}{R}\right) p \frac{\partial r}{\partial n} = 0 \quad . \quad (C-4) \end{aligned}$$

From the geometry of the shock layer, referring to Fig. 1, it can be seen that

$$dr = \left(1 + \frac{n}{R}\right) \sin\theta \, ds + \cos\theta \, dn \quad . \quad (C-5)$$

Thus,

$$\frac{dr}{dn} = \cos\theta \quad . \quad (C-6)$$

Using this result and Eqs. (A-3) in Eq. (C-4), it is found that the n-momentum equation becomes

$$\begin{aligned} \frac{\partial}{\partial s} (r z) + \frac{\partial}{\partial n} \left[\left(1 + \frac{n}{R}\right) r h \right] - \frac{r}{R} g \\ - \left(\frac{\gamma-1}{2\gamma}\right) \left(1 + \frac{n}{R}\right) p \cos\theta = 0 \quad . \quad (C-7) \end{aligned}$$

Knowing that

$$\frac{p}{\rho} = 1 - w^2 = 1 - (u^2 + v^2) \quad (C-8)$$

and

$$\frac{p}{\rho^2} = \phi \quad (C-9)$$

then the above four equations, Eqs. (C-3), (C-7), (C-8), and

(C-9) can be used to determine the four unknowns u , v , p , and ρ , provided that the variation of ϕ with respect to the stream function is known.

Eqs. (C-3) and (C-7) can be integrated with respect to n across the shock layer, from $n = 0$ to $n = \delta$.

By the use of Leibnitz's rule, i.e.,

$$\frac{d}{ds} \int_0^{g(s)} F(n,s) dn = \int_0^{g(s)} \frac{\partial F}{\partial s} dn + F[g(s),s] \frac{dg(s)}{ds}$$

or

$$\int_0^{g(s)} \frac{\partial F}{\partial s} dn = \frac{d}{ds} \int_0^{g(s)} F(n,s) dn - F[g(s),s] \frac{dg(s)}{ds} \quad (C-10)$$

and knowing the conditions on the body surface, i.e.,

$v_0 = 0$, $h_0 = 0$, and $z_0 = 0$, then

$$\left(1 + \frac{\delta}{R}\right) r_1 h_1 - r_1 t_1 \frac{d\delta}{ds} + \frac{d}{ds} \int_0^{\delta} (rt) dn = 0 \quad (C-11)$$

and

$$\begin{aligned} \frac{d}{ds} \int_0^{\delta} (rz) dz - r_1 z_1 \frac{d\delta}{ds} + \left(1 + \frac{\delta}{R}\right) r_1 H_1 - r_0 H_0 \\ - \int_0^{\delta} \left(\frac{r}{R}\right) g dn - \left(\frac{\gamma-1}{\gamma}\right) \cos\theta \int_0^{\delta} \left(1 + \frac{n}{R}\right) p dn = 0 \end{aligned} \quad (C-12)$$

Now, suppose that the variation of the integrands in the above two equations are known, so that these integrands are given in terms of their values at the boundaries; that

is, body surface and the shock. Then these equations would be ordinary differential equations (with s as the independent variable) containing δ , u_1 , v_1 , u_0 , v_0 , ϕ_1 , and ϕ_0 . But $v_0 = 0$ and, since the body surface is also a streamline, $\phi_0 = \phi_{sp}$ is known from normal shock relations. From oblique shock relations one can find u_1 , v_1 , and ϕ_1 as functions of x . Therefore, we now have three unknown variables, i.e., δ , x and u_0 . In addition to Eqs. (C-3) and (C-7) one more equation is needed. This can be acquired from the relation between δ and x as noted from the geometry of Fig. 1:

$$\frac{ds'}{d\delta} = \cot\left[\frac{\pi}{2} - (\theta + x)\right] = \tan(\theta + x)$$

and

$$\frac{ds}{ds'} = \frac{R}{R+\delta} = \frac{1}{1 + \frac{\delta}{R}}$$

Here ds' is an incremental line element along the shock corresponding to ds along the body.

Multiplying the above two equations together the following desired relation follows; namely,

$$\frac{d\delta}{ds} = \left(1 + \frac{\delta}{R}\right) \cot\theta \quad . \quad (C-13)$$

The simultaneous numerical solution of the three differential Eqs. (C-3), (C-7), and (C-13) will determine local shock-layer thickness δ , the shock shape parameter x , and the velocity distribution along the body surface, u_0 . All of these quantities are given in terms of the local body

distance s , the single independent variable in these relations.

(D) Oblique Shock Relations

The values of u_1 , v_1 , and ϕ_1 , immediately behind the shock, are related to the shock inclination angle, $(\pi/2 - \alpha)$, by the known oblique shock relations. In the present coordinate system and with non-dimensional quantities, these relations take on special forms as derived below:

$$\phi_1 = \frac{p_1}{\rho_1^\gamma} = \left(\frac{p_1'}{p_0'}\right) \left(\frac{\rho_0'}{\rho_1'}\right)^\gamma .$$

But

$$\frac{p_1'}{\rho_1^\gamma} = \text{constant} = \frac{p_\infty'}{\rho_\infty^\gamma} .$$

Thus

$$\phi_1 = \left(\frac{p_1'}{p_\infty'}\right) \left(\frac{\rho_\infty'}{\rho_1'}\right)^\gamma .$$

From (Ref. 1)

$$\frac{p_1'}{p_\infty'} = \frac{2\gamma M_\infty^2 \cos^2 \alpha - (\gamma - 1)}{\gamma + 1}$$

and

$$\frac{\rho_\infty'}{\rho_1'} = \frac{2 + (\gamma - 1)M_\infty^2 \cos^2 \alpha}{(\gamma + 1)M_\infty^2 \cos^2 \alpha} .$$

Thus

$$\phi_1 = \left[\frac{2\gamma M_\infty^2 \cos^2 x - (\gamma-1)}{\gamma+1} \right] \times \left[\frac{2 + (\gamma-1)M_\infty^2 \cos^2 x}{(\gamma+1)M_\infty^2 \cos^2 x} \right] \quad (D-1)$$

Because the surface of the body is a streamline, then, by knowing that $x = 0$ along the body proper,

$$\phi_0 = \left[\frac{2\gamma M_\infty^2 - (\gamma-1)}{\gamma+1} \right] \times \left[\frac{2 + (\gamma-1)M_\infty^2}{(\gamma+1)M_\infty^2} \right] \quad (D-2)$$

Next, with the non-dimensional freestream velocity as (Ref. 1)

$$\begin{aligned} w_\infty &= \frac{w_\infty^f}{V_{\max}^f} = \left[\left(\frac{\gamma-1}{2} \right) M_\infty^2 \left(1 + \frac{\gamma-1}{2} M_\infty^2 \right)^{-1} \right]^{\frac{1}{2}} \\ &= M_\infty \sqrt{\frac{\gamma-1}{2 + (\gamma-1)M_\infty^2}} \quad (D-3) \end{aligned}$$

The velocity components immediately behind the shock are derived as follows:

$$\frac{w_1}{w_\infty} = \frac{w_1^f / V_{\max}^f}{w_\infty^f / V_{\max}^f} = \frac{w_1^f}{w_\infty^f}$$

or

$$w_1 = w_\infty \left(\frac{w_1^f}{w_\infty^f} \right)$$

From Eqs. (136) and (138) of Ref. 1, we have

$$w_1 = w_\infty \left[1 - \frac{4(M_\infty^2 \cos^2 x - 1)(\gamma - M_\infty^2 \cos^2 x + 1)}{(\gamma+1)^2 M_\infty^4 \cos^2 x} \right]^{\frac{1}{2}} \quad (D-4)$$

and

$$\cot \alpha = \left[\frac{(\gamma+1)M_\infty^2}{2(M_\infty^2 \cos^2 x - 1)} - 1 \right] \cot x \quad (D-5)$$

Referring to Fig. 1,

$$\begin{aligned} \tan \sigma &= \tan \left[\frac{\pi}{2} - (\theta - \alpha) \right] = \cot(\theta - \alpha) \\ &= \frac{\cot \theta \cot \alpha + 1}{\cot \alpha - \cot \theta} \quad (D-6) \end{aligned}$$

Now, substituting Eq. (D-5) into Eq. (D-6) then after rearranging,

$$\begin{aligned} \tan \sigma &= \left\{ \left[1 - \frac{2}{\gamma+1} \left(\cos^2 x - \frac{1}{M_\infty^2} \right) \right] \cos \theta \right. \\ &\quad \left. + \left[\frac{2}{\gamma+1} \tan x \left(\cos^2 x - \frac{1}{M_\infty^2} \right) \right] \sin \theta \right\} / \left\{ \left[1 - \frac{2}{\gamma+1} \left(\cos^2 x - \frac{1}{M_\infty^2} \right) \right] \sin \theta \right. \\ &\quad \left. - \left[\frac{2}{\gamma+1} \tan x \left(\cos^2 x - \frac{1}{M_\infty^2} \right) \right] \cos \theta \right\} \end{aligned}$$

and hence

$$\begin{aligned} \sin \sigma &= \left\{ \left[1 - \frac{2}{\gamma+1} \left(\cos^2 x - \frac{1}{M_\infty^2} \right) \right] \cos \theta \right. \\ &\quad \left. + \left[\frac{2}{\gamma+1} \tan x \left(\cos^2 x - \frac{1}{M_\infty^2} \right) \right] \sin \theta \right\} / \left\{ \left[1 - \frac{2}{\gamma+1} \left(\cos^2 x - \frac{1}{M_\infty^2} \right) \right]^2 \right. \\ &\quad \left. + \left[\frac{2}{\gamma+1} \tan x \left(\cos^2 x - \frac{1}{M_\infty^2} \right) \right]^2 \right\}^{\frac{1}{2}} \quad (D-7) \end{aligned}$$

It should be noted that the denominator of the above equation can be rewritten as

$$\left\{ 1 - \frac{4(M_\infty^2 \cos^2 x - 1)(\gamma M_\infty^2 \cos^2 x + 1)}{(\gamma+1)^2 M_\infty^2 \cos^2 x} \right\}^{\frac{1}{2}} \quad (D-8)$$

Now using Eqs. (D-4) and (D-7) with (D-8), the velocity component immediately behind the shock and parallel to the body is, then,

$$u_1 = w_1 \sin \sigma = w_\infty \left\{ \left[1 - \frac{2}{\gamma+1} \left(\cos^2 x - \frac{1}{M_\infty^2} \right) \right] \cos \theta + \left[\frac{2}{\gamma+1} \tan x \left(\cos^2 x - \frac{1}{M_\infty^2} \right) \right] \sin \theta \right\} \quad (D-9)$$

Similarly, the normal velocity component is

$$v_1 = w_1 \cos \sigma = w_\infty \left\{ \left[1 - \frac{2}{\gamma+1} \left(\cos^2 x - \frac{1}{M_\infty^2} \right) \right] (-\sin \theta) + \left[\frac{2}{\gamma+1} \tan x \left(\cos^2 x - \frac{1}{M_\infty^2} \right) \right] \cos \theta \right\} \quad (D-10)$$

Finally, the pressure on the body surface can be obtained from Eqs. (B-10) and (D-2); that is,

$$\begin{aligned} p_0 &= (1-u_0^2)^{\frac{\gamma}{\gamma-1}} \phi_0 \frac{1}{\gamma-1} \\ &= (1-u_0^2)^{\frac{\gamma}{\gamma-1}} \left\{ \left[\frac{2\gamma M_\infty^2 - (\gamma-1)}{\gamma+1} \right] \left[\frac{2+(\gamma-1)M_\infty^2}{(\gamma+1)M_\infty^2} \right]^\gamma \right\}^{\frac{1}{\gamma-1}} \\ &= \left[(1-u_0^2)^{\frac{\gamma}{\gamma-1}} \frac{(\gamma+1)M_\infty^2}{2+(\gamma-1)M_\infty^2} \right]^{\frac{\gamma}{\gamma-1}} \left[\frac{2\gamma M_\infty^2 - (\gamma-1)}{\gamma+1} \right]^{\frac{1}{\gamma-1}} \end{aligned}$$

(D-11)

(E) Applying the First Approximation

Only the first approximation to the problem is considered in this thesis. According to Belotserkovskii this can be achieved by assuming the integrand for the integrated continuity and n-momentum equations, i.e., Eqs. (C-11) and (C-12), to be linear in n.

Suppose the integrand is of the form, $F(n,s)$. Then the assumption of linearity requires that

$$F(n,s) = (F_0,s) + \frac{n}{\delta} [F(\delta,s) - F(0,s)] \quad , \quad (E-1)$$

and the integration of the function across the shock layer becomes

$$\begin{aligned} \int_0^\delta F(n,s)dn &= \int_0^\delta \left\{ F(0,s) + \frac{n}{\delta} [F(\delta,s) - F(0,s)] \right\} dn \\ &= \frac{\delta}{2} [F(\delta,s) + F(0,s)] = \frac{\delta}{2} [F_1(s) + F_0(s)] . \end{aligned} \quad (E-2)$$

The subscripts 0 and 1 (here) indicate the evaluation at the body surface and at the shock, respectively. By use of Eq. (E-2), the four integrations appearing in Eqs. (C-11) and (C-12) can be rewritten as follows:

$$\begin{aligned} (1) \quad \frac{d}{ds} \int_0^\delta (rt)dn &= \frac{d}{ds} \left\{ \frac{\delta}{2} [(rt)_1 + (rt)_0] \right\} \\ &= \frac{1}{2} [(rt)_1 + (rt)_0] \frac{d\delta}{ds} + \frac{\delta}{2} \frac{d}{ds} [(rt)_1 \\ &\quad + (rt)_0] \end{aligned} \quad (E-3)$$

where

$$(rt)_0 = r_0 (1 - u_0^2)^{\frac{1}{\gamma-1}} u_0$$

and

$$(rt)_1 = (r_0 + \delta \cos \theta) (1 - w_1^2)^{\frac{1}{\gamma-1}} u_1 \quad ;$$

$$\begin{aligned} (2) \quad \frac{d}{ds} \int_0^\delta (rz) dn &= \frac{d}{ds} \left\{ \frac{\delta}{2} [(rz)_1 + (rz)_0] \right\} \\ &= \frac{1}{2} [(rz)_1 + (rz)_0] \frac{d\delta}{ds} \\ &\quad + \frac{\delta}{2} \frac{d}{ds} [(rz)_1 + (rz)_0] \end{aligned} \quad (E-4)$$

where

$$(rz)_0 = r_0 \rho_0 u_0 v_0 = 0$$

and

$$(rz)_1 = (r_0 + \delta \cos \theta) \rho_1 u_1 v_1 \quad ;$$

$$\begin{aligned} (3) \quad \int_0^\delta \left(\frac{r}{R} \right) g dn &= \frac{\delta}{2} \left\{ \left[\left(\frac{r}{R} \right) g \right]_1 + \left[\left(\frac{r}{R} \right) g \right]_0 \right\} \\ &= \frac{\delta}{2} \frac{(r_0 + \delta \cos \theta)}{R} g_1 + \frac{\delta}{2} \frac{r_0}{R} g_0 \end{aligned} \quad (E-5)$$

where

$$g_1 = \rho_1 u_1^2 + \frac{\gamma-1}{2\gamma} p_1$$

and

$$g_0 = \rho_0 u_0^2 + \frac{\gamma-1}{2\gamma} p_0 \quad ;$$

and

$$\begin{aligned}
 (4) \quad \int_0^{\delta} \left(1 + \frac{n}{R}\right) p \, dn &= \frac{\delta}{2} \left[\left(1 + \frac{n}{R}\right) p\right]_1 + \frac{\delta}{2} \left[\left(1 + \frac{n}{R}\right) p\right]_0 \\
 &= \frac{\delta}{2} \left[\left(1 + \frac{\delta}{R}\right) p_1 + p_0\right] \quad . \quad (E-6)
 \end{aligned}$$

The terms p_1 , p_0 , ρ_1 , and ρ_0 are obtained from Eqs. (C-13) and (C-14), and are

$$\begin{aligned}
 p_1 &= (1 - w_1^2)^{\frac{\gamma}{\gamma-1}} \phi_1^{-\frac{1}{\gamma-1}} \\
 \rho_1 &= (1 - w_1^2)^{\frac{1}{\gamma-1}} \phi_1^{-\frac{1}{\gamma-1}} \\
 p_0 &= (1 - u_0^2)^{\frac{\gamma}{\gamma-1}} \phi_0^{-\frac{1}{\gamma-1}} \\
 \rho_0 &= (1 - u_0^2)^{\frac{1}{\gamma-1}} \phi_0^{-\frac{1}{\gamma-1}}
 \end{aligned} \quad (E-7)$$

respectively.

Substituting Eqs. (E-3) through (E-7) into Eqs. (C-11) and (C-12) and making use of the oblique shock relations (D-1), (D-2), (D-9) and (D-10), then carrying out all the differentiations, (together with Eqs. (C-13)), three first-order total differential equations result. The expressions contain δ , x and u_0 and their derivatives with respect to s as unknowns. The manipulation is very lengthy and painstaking requiring many pages to write down; therefore, the details will be omitted here.

The resulting three differential equations are solved for the derivatives of δ , u_0 and x in the following form

$$\frac{d\delta}{ds} = \left(1 + \frac{\delta}{R}\right) \cot(\theta + \alpha) \quad (E-8)$$

$$\frac{du_0}{ds} = \frac{1}{B} \left\{ D - A \left(\frac{d\delta}{ds} \right) - \frac{C}{F} \left[G + E \left(\frac{d\delta}{ds} \right) \right] \right\} \quad (E-9)$$

$$\frac{dx}{ds} = \frac{1}{F} \left[G + E \left(\frac{d\delta}{ds} \right) \right] \quad (E-10)$$

where A, B, C, D, E, F and G are given as follows:*

$$A = \frac{r_0}{2} \left[u_0 (1 - u_0^2)^{\frac{1}{\gamma-1}} - u_1 (1 - w_1^2)^{\frac{1}{\gamma-1}} \right]$$

$$B = \frac{r_0 \delta}{2} (1 - u_0^2)^{\frac{2-\gamma}{\gamma-1}} \left[1 - \frac{\gamma+1}{\gamma-1} u_0^2 \right]$$

$$C = \frac{2\gamma}{\gamma+1} (r_0 + \delta \cos\theta) (1 - w_1^2)^{\frac{1}{\gamma-1}} w_\infty$$

$$\times \left[\left[1 - \frac{2u_1^2}{(\gamma-1)(1-w_1^2)} \right] \left\{ \left[\frac{1}{2} \left(1 - \frac{1}{M_\infty^2 \cos^2 \alpha} \right) - \sin^2 \alpha \right] \sin\theta \right. \right.$$

$$\left. \left. + (\sin \alpha \cos \alpha) \cos\theta \right\} - \left[\frac{2u_1 v_1}{(\gamma-1)(1-w_1^2)} \right] \right.$$

$$\left. \times \left\{ \left[\frac{1}{2} \left(1 - \frac{1}{M_\infty^2 \cos^2 \alpha} \right) - \sin^2 \alpha \right] \cos\theta - (\sin \alpha \cos \alpha) \sin\theta \right\} \right]$$

$$D = -\left(1 + \frac{\delta}{2R}\right) (r_0 + \delta \cos\theta) (1 - w_1^2)^{\frac{1}{\gamma-1}} v_1$$

$$- \frac{1}{2} \delta \sin\theta \left[(1 - u_0^2)^{\frac{1}{\gamma-1}} u_0 + (1 - w_1^2)^{\frac{1}{\gamma-1}} u_1 \left(1 + \frac{\delta}{R}\right) \right]$$

* In Traugott's paper (Ref. 19), the last $\cos\theta$ appearing in his expression for C seems to be a typographical error for $\sin\theta$, according to the author's derivation.

$$E = \frac{1}{2} r_0 \rho_1 u_1 v_1$$

$$F = \frac{2}{\gamma+1} \delta (r_0 + \delta \cos \theta) \rho_1 w_\infty \left[v_1 \left[1 - \frac{2u_1^2}{(\gamma-1)(1-w_1^2)} \right] \right. \\ \times \left\{ \left[\frac{1}{2} \left(1 - \frac{1}{M_\infty^2 \cos^2 x} \right) - \sin^2 x \right] \sin \theta + (\sin x \cos x) \cos \theta \right\} \\ + u_1 \left[1 - \frac{2v_1^2}{(\gamma-1)(1-w_1^2)} \right] \\ \times \left\{ \left[\frac{1}{2} \left(1 - \frac{1}{M_\infty^2 \cos^2 x} \right) - \sin^2 x \right] \cos \theta - (\sin x \cos x) \sin \theta \right\} \Big] \\ + \left(\frac{\gamma}{\gamma+1} \right) (r_0 + \delta \cos \theta) \rho_1^{1-\gamma} \phi_1^{-1} u_1 v_1 \tan x \frac{(M_\infty^2 \cos^2 x - 1)^2}{2 + (\gamma-1) M_\infty^2 \cos^2 x}$$

and

$$G = -\rho_1 \left\{ v_1^2 \left(1 + \frac{\delta}{2R} \right) (r_0 + \delta \cos \theta) + u_1 v_1 \left(1 + \frac{\delta}{R} \right) \frac{\delta}{2} \sin \theta \right\} \\ + \frac{1}{2R} \rho_0 u_0^2 r_0 \delta - \frac{\gamma-1}{2\gamma} (r_0 + \frac{\delta}{2} \cos \theta + \frac{\delta}{2R} r_0) (p_1 - p_0) \quad . \\ (E-11)$$

(F) Geometry of the Paraboloid of Revolution

The flow field to be considered here will be that past a paraboloid of revolution. The equation of the body surface, in the meridian plane, is

$$r_0'^2 = 2R_{sp}' X' \quad (F-1)$$

or in non-dimensional form

$$r_0^2 = 2X \quad . \quad (F-2)$$

Now, an incremental line element along the body surface is described by

$$ds = \sqrt{(dr_0)^2 + (dX)^2} \quad ,$$

hence

$$\begin{aligned} s &= \int_0^X ds = \int_0^X \sqrt{\frac{1+2X}{2X}} dX \\ &= \sqrt{X\left(\frac{1}{2} + X\right)} + \frac{1}{2} \ln \left| \frac{\sqrt{X} + \sqrt{\frac{1}{2} + X}}{\sqrt{\frac{1}{2}}} \right| \quad . \quad (F-3) \end{aligned}$$

From Eq. (F-2)

$$r_0 = \cot \theta \quad \text{and} \quad X = \frac{1}{2} \cot^2 \theta \quad . \quad (F-4)$$

Thus, we have the following relation between x and θ for the paraboloid:

$$s = \frac{\cos \theta}{2 \sin^2 \theta} + \frac{1}{2} \ln \left(\frac{1 + \cos \theta}{\sin \theta} \right) \quad . \quad (F-5)$$

Next, the radius of curvature of the body surface at any s (or θ) is given by

$$R = \frac{1}{-\frac{d\theta}{ds}} = -\frac{ds}{d\theta} = \sin^{-3} \theta \quad . \quad (F-6)$$

It should be noted that Eqs. (F-4) through (F-6) are all implicit functions in the sense that s is the independent variable instead of θ . Therefore, the value of θ for a given value of s can be found only by an iterative procedure.

(G) Boundary Conditions and the Methods of Solving the Differential Equations

Substituting the values of A through G (see Eq. (E-11)) into Eqs. (E-8), (E-9) and (E-10), it is apparent that these equations can be expressed in the form

$$\begin{aligned}\frac{d\delta}{ds} &= f_1(\delta, x, \theta, R) \\ \frac{du_0}{ds} &= f_2(\delta, x, \theta, R, r_0, \gamma, M_\infty) \\ \frac{dx}{ds} &= f_3(\delta, x, \theta, R, r_0, \gamma, M_\infty)\end{aligned}\quad (G-1)$$

In these equations γ and M_∞ will be given for a particular problem. The quantities θ , R and r_0 are geometrical features of the body (given in terms of s), and (hence) become fixed once the body shape is known. We also note that the three unknown variables appear in all three differential equations, so that Eqs. (G-1) are coupled non-linear first-order differential equations. It appears that these equations are impossible to solve analytically; however, they may be solved numerically.

To start the integration of these equations by a finite difference process, it is necessary to know initial values for δ , u_0 and x . By the symmetry of the flow field these initial conditions are, at $s = 0$,

$$\delta = \delta_{sp}, \quad u_0 = 0, \quad \text{and} \quad x = 0 \quad (G-2)$$

But the stagnation-point shock detachment distance, δ_{sp} , is

actually unknown a priori; δ_{sp} must be determined as a part of the problem.

From Eqs. (E-9) and (E-10) it can be seen that both derivatives become infinite as F vanishes. Also,

$\frac{du_0}{ds}$ alone will become infinite when B vanishes. Now, at the stagnation point F is equal to zero, while C, G, and E are also zero. It follows that both terms containing F in the denominator (i.e., $\frac{C}{F}[G + E(\frac{d\delta}{ds})]$ and $\frac{1}{F}[G + E(\frac{d\delta}{ds})]$) become indeterminate at the stagnation point. Fortunately, even without devising a process to settle this indeterminacy at $s = 0$, the calculated results show only a small jump at the first step of a finite difference process. Thereafter, the value of F decreases steadily as s increases, while in the vicinity of the sonic point on the body surface it increases slightly but still remains negative. Although there is no physical interpretation for the quantity F, it is safe to say that its vanishing does not occur within the region of interest along s (except at the stagnation point itself).

Next, consider the vanishing of B. The quantity B will vanish when

$$u_0 = \sqrt{\frac{\gamma-1}{\gamma+1}},$$

as seen from Eq. (E-9). This means that $B = 0$ when the velocity along the body surface reaches the sonic velocity

(see Eq. (D-3)). In physical reality, the velocity derivative at the sonic point should remain finite, so that both the numerator and the denominator of Eq. (E-9) have to vanish at the sonic point. That is, when $B = 0$,

$$D - A\left(\frac{ds}{ds}\right) - \frac{C}{F}\left[G + E\left(\frac{ds}{ds}\right)\right] = 0 \quad . \quad (G-4)$$

This additional condition is used to determine δ_{sp} by means of an iterative procedure. It is possible that an infinite velocity gradient does physically occur on the body surface when an abrupt change in profile exists. However, it will not occur in the present case for the flow past a paraboloid of revolution.

V. METHODS AND DISCUSSION OF COMPUTER CALCULATION

In order to solve the system of equations (E-8), (E-9) and (E-10), subject to the initial conditions (G-2), where δ_{sp} is some estimated value, an electronic computer program has been devised. With the estimated δ_{sp} , the computation begins at stagnation point and proceeds to the sonic point, (where $u_0 = \sqrt{(\gamma-1)/(\gamma+1)}$) and where the value of the left hand side of (G-4) is checked. For brevity this value will be denoted by Δ hereafter. This series of calculation is referred to as one iteration.

If Δ varies significantly from zero, a new value of δ_{sp} is chosen. This procedure is repeated until a value of δ_{sp} is obtained such that Δ is within some specified range of accuracy.

A typical case, at $M_\infty = 3$ and $\gamma = 1.4$, for the variation of Δ versus u_0 is shown in Fig. 3. It can be seen that for the correctly estimated δ_{sp} , denoted by curve (3), the value of Δ increases from zero and reaches a maximum where u_0 is about one half of its sonic speed. Subsequently Δ decreases, reaching a value of zero when u_0 has increased to the sonic speed. If the estimated value of δ_{sp} is too small, then Δ diverges quite rapidly as u_0 approached sonic speed; this is illustrated by curve (1) and (3) of Fig. 3. On the other hand, if the estimated value of δ_{sp} is too

large, then Δ will decrease to zero and takes on negative value before u_0 reaches the sonic value; this is illustrated by curve (4) and (5) of Fig. 3. Since δ_{sp} for curve (2) is only 0.0001 smaller than δ_{sp} for curve (3), and δ_{sp} for curve (4) is only 0.0001 larger than δ_{sp} for curve (3), it may be concluded that variations in Δ are extremely sensitive to the selection of a proper value for δ_{sp} . Actually, this behavior of Δ is used as a guide for improving the estimated value of δ_{sp} in the iterative procedure.

The computer program was first written using a fourth-order Runge-Kutta integration scheme to carry out numerical integration of Eqs. (E-8), (E-9) and (E-10). It was found that approximately 40,000 core storage positions were needed, which exceeded the capacity of the basic IBM 1620 electronic computer. Therefore, an IBM 1620 with an added IBM 1623 Core Storage Unit was used. Subsequently the Runge-Kutta program proved to be very time consuming and was rewritten. The new program simply proceeded stepwise along the body, in Δs increments, without benefit of the averaging features of the Runge-Kutta method. Although the program was reduced to half the size of the former one, it still required about 25,000 core storage positions, and again exceeded the basic IBM 1620 computer capacity. Mathematically, the former method should be more accurate than the latter one, yet the results of these two methods showed no significant

differences. This is not surprising, when it is noted that variations of all dependent variables, δ , u_0 and x , with respect to s , are nearly linear, at least in the range of interest, (i.e., from the stagnation point to the sonic point).

The computer running time for each iteration depends upon the increment size of the independent variable s . With the present computer program, using the non-averaging step-wise integration, each iteration requires about ten minutes of running time, with about 20 steps needed to reach the sonic point.

As for the number of iterations needed to secure a specified accuracy, this depends somewhat on the experience of the operator and on whether or not good starting estimates for δ_{sp} are available. (These could be obtained from experimental data, theoretical approximation, and/or other sources.) Usually seven to eight iterations are needed for an accuracy in δ_{sp} to within three significant figures, i.e., to one thousandth of the radius of the nose curvature.

Because of the sensitivity of the solution at the sonic point, the step located one interval upstream of the sonic point is used as that station for checking values of Δ while iterating on values of δ_{sp} . When the correct value of δ_{sp} is obtained the flow quantities at that station are extrapolated in order to obtain the conditions at the sonic point.

VI. DISCUSSION OF CALCULATED RESULTS

The flow of an ideal diatomic gas ($\gamma = 1.4$) past paraboloids of revolution at $M_\infty = 3, 4, 6, 10$ and 1000 , and for an ideal monatomic gas at $M_\infty = 3, 6$ and 10 have been computed using the first approximation of the integral-relations method. Since for the completely supersonic region these are more accurate methods, such as the method of characteristics, the calculations were carried only slightly beyond the sonic line.

The calculated shock shapes and associated sonic lines, for $\gamma = 1.4$, are shown in Fig. 4 and for $\gamma = 5/3$ in Fig. 5. The velocity variations along the body surface are shown in Fig. 6 for $\gamma = 1.4$, and in Fig. 7 for $\gamma = 5/3$. Pressure distributions along the body are shown in Fig. 8 for $\gamma = 1.4$ and in Fig. 9 for $\gamma = 5/3$.

Unfortunately, no experimental data have been found for the supersonic flow of a gas past paraboloids of revolution. Thus, the present calculated results are compared only with calculated quantities obtained by Van Dyke's inverse method (Ref. 24). The comparison of Van Dyke's results prove to be in good agreement with experiments for the case of supersonic and hypersonic flow past spheres; therefore, the corresponding calculated values for the flow past paraboloids is presumed to be a good criterion.

The stagnation shock detachment distances, as computed by the integral-relations method, are found to be very close to the values obtained from Van Dyke's method. At $M_\infty = 3$ the difference is within 5% of Van Dyke's values, and at $M_\infty = 10$ the difference is only 4%. For a fixed value of γ , the shock detachment distance decreases rapidly with an increase in M_∞ , for values of M_∞ less than 4. The differences become smaller at higher values of M_∞ . For example, with $\gamma = 1.4$, the change in δ_{sp} is only 5% when M_∞ is increased from $M_\infty = 10$ to $M_\infty = 1000$. In other words, the shock shape has closely approached its asymptotic position when the free-stream Mach number equals to 10. This has been predicted by the Mach number independence principle (Ref. 11).

At a fixed Mach number, δ_{sp} increases rapidly as γ increases. The ratio of δ_{sp} for $\gamma = 5/3$ to that at $\gamma = 1.4$, at $M_\infty = 10$, is 1.55 which is in good agreement compared to the limiting value that can be predicted analytically, namely:

$$\left(\frac{5/3 - 1}{5/3 + 1}\right) / \left(\frac{1.4 - 1}{1.4 + 1}\right) = 1.50 \quad .$$

The sonic-line locations as determined by the integral-relations method, lie very close to those given by Van Dyke (see Figs. 4 and 5). All the sonic lines lean upstream as they emerge from the paraboloid proper.

The tendency of leaning upstream increases as the Mach number increases, or as γ decreases. The sonic point, on

the body, moves downstream quite rapidly at small M_∞ and for a fixed γ . As shown in Van Dyke's paper (Ref. 24), at $M_\infty = 2$, the sonic line does not meet the body until very far downstream from the stagnation point. But, since the sonic condition is the most important condition for the utility of the integral-relations method, it is clear that the integral-relations method is not suitable for application to a flow past a paraboloid at M_∞ equal or less than 2. Here we see one of the principal differences between the flow past paraboloids and spheres. For flow past spheres the sonic point, on the body, is located very nearly 45° away from the stagnation point (at any Mach number), and the sonic line leans downstream at a low value of M_∞ .

In Figs. 6 and 7, the velocity variation along the body is seen to be nearly linear up to the sonic point.

The pressure distribution, along the body, as calculated by the integral-relations method agrees very well with Van Dyke's results. These results are also compared with the Newtonian simple impact theory (i.e., without centrifugal correction). At $M_\infty = 10$, the calculated value is slightly smaller than that predicted by simple impact theory (for $\gamma = 1.4$) and is slightly larger for $\gamma = 5/3$, as shown in Figs. 8 and 9.

VII. CONCLUSIONS

After judging the results presented in this thesis, several conclusions have been reached:

(1) For supersonic and hypersonic flow past paraboloids of revolution, the shock shapes, shock detachment distances, sonic line locations and pressure distributions calculated by the first approximation of the integral-relations method are in good agreement with results obtained by Van Dyke's inverse method. The agreement becomes better as the freestream Mach numbers increase, while the method appears unsuitable at M_∞ values less than 2.

(2) For better accuracy the second approximation of the integral-relations method is needed. However, the second approximation will exceed the capacity of an IBM 1620 computer even when including the additional IBM 1623 Core Storage Unit.

(3) The sensitivity of the method to a slight error in the estimated stagnation shock detachment distance requires the accuracy of the estimated value of δ_{sp} to be within at least 10^{-4} . Thus, electronic computers with higher speed than IBM 1620 would be highly desirable when using the integral-relations method.

VIII. SUMMARY

Under the assumption of an ideal gas with constant specific heat ratio, the first approximation of the integral-relations method, which considers the entire shock layer as a single strip, is derived for axisymmetric bodies of arbitrary, smooth contours, following a development similar to that of S. C. Traugott. The assumption of a linear variation for certain of the flow variables across the shock is used. The resulting ordinary differential equations are integrated, using a numerical scheme, over paraboloids of revolution at supersonic and hypersonic speeds. The shock shapes, shock detachment distances, location of sonic lines, velocity variations, and pressure distributions along the body surface are calculated for ideal diatomic gases (with $\gamma = 1.4$) at $M_\infty = 3, 4, 6, 10$ and 1000 ; and for monoatomic gases (with $\gamma = 5/3$) at $M_\infty = 3, 6$ and 10 . These calculations were obtained on an IBM 1620 computer which included an additional IBM 1623 Core Storage Unit. The calculated results were compared with those obtained by Van Dyke's inverse method. Agreement was found to be good, considering that only the first approximation of the integral-relations method was used.

IX. ACKNOWLEDGEMENTS

The author should like to express his sincere gratitude to _____, for his many inspiring suggestions leading to the successful completion of this thesis. _____ encouragement and patience were especially appreciated when the author encountered difficulties in the computer calculations.

The author also desires to express his thanks to _____, for his help in obtaining several important references for this thesis, as well as his enlightening instruction and concern during the author's one and a half years study at Virginia Polytechnic Institute.

X. BIBLIOGRAPHY

1. Ames Research Staff. EQUATIONS, TABLES AND CHARTS FOR COMPRESSIBLE FLOW. NACA Report 1135, 1953.
2. Belotserkovskii, O. M. FLOW WITH A DETACHED SHOCK WAVE ABOUT A SYMMETRIC PROFILE. Journal of Applied Mathematics and Mechanics, Vol. 22, No. 2, Pergamon Press Inc., 1958.
3. Belotserkovskii, O. M. ON THE CALCULATION OF FLOW PAST AXISYMMETRIC BODIES WITH DETACHED SHOCK WAVES USING A ELECTRONIC COMPUTING MACHINE. Journal of Applied Mathematics and Mechanics, Vol. 24, No. 3, Pergamon Press Inc., 1960.
4. Busemann, A. A REVIEW OF ANALYTICAL METHODS FOR THE TREATMENT OF FLOWS WITH DETACHED SHOCKS. NACA TN 1858, April 1949.
5. Chester, W. SUPERSONIC FLOW PAST A BLUFF BODY WITH A DETACHED SHOCK, Part II. Journal of Fluid Mechanics, Vol. I, part 5, p. 490, November, 1956.
6. Chushkin, P. I. SUPERSONIC FLOWS AROUND BLUNTED BODIES OF SIMPLE SHAPE. Journal of Applied Mathematics and Mechanics, Vol. 24, No. 5, 1960.
7. Doroniteyn, A. A. A CONTRIBUTION TO THE SOLUTION OF MIXED PROBLEMS OF TRANSONIC AERODYNAMICS. Advances in Aeronautical Sciences, Vol. 2, pp. 832-844, Pergamon Press Inc., 1959.
8. Freeman, N. C. ON THE THEORY OF HYPERSONIC FLOW PAST PLANE AND AXIALLY SYMMETRIC BODIES. Journal of Fluid Mechanics, Vol. I, pp. 366-387, 1956.
9. Gold, R., and Holt, M. CALCULATION OF SUPERSONIC FLOW PAST A FLAT-HEADED CYLINDER BY BELOTSEKOVSKII'S METHOD. Division of Applied Mathematics, Brown University, AFOSR TN-59-199, March 1959.
10. Goldstein, S. MODERN DEVELOPMENTS IN THE FLUID DYNAMICS. Vol. I, Oxford Press, 1950.
11. Hayes, W. D., and Probstein, R. F. HYPERSONIC FLOW THEORY. The Johns Hopkins University, 1959.

12. Holt, M. DIRECT CALCULATION OF PRESSURE DISTRIBUTION ON BLUNT HYPERSONIC NOSE SHAPES WITH SHARP CORNER. Journal of Aerospace Sciences, Vol. 28, No. 11, pp. 872-877, November 1961.
13. Levy, H., and Baggott, E. A. NUMERICAL SOLUTION OF DIFFERENTIAL EQUATIONS. Dover Publication Inc., 1950.
14. Maccoll, J. W., and Codd, J. THEORETICAL INVESTIGATIONS OF THE FLOW AROUND VARIOUS BODIES IN THE SONIC REGION OF VELOCITIES. Theoretical Research Report No. 17/45, Armament Research Department, Ministry of Supply, Fort Halstead, Kentucky, 1945.
15. Maslen, S. H., and Moeckel, W. E. INVICID HYPERSONIC FLOW PAST BLUNT BODIES. Journal of Aeronautical Sciences, Vol. 24, No. 9, September 1957.
16. Mitchell, A. R. APPLICATION OF RELAXATION TO THE ROTATIONAL FIELD OF FLOW BEHIND A BOW SHOCK WAVE. Quarterly Journal of Mechanics and Applied Mathematics, Vol. 4, pp. 371-383, 1951.
17. Probststein, R. F. ON THE NATURE OF THE SONIC LINE FOR SUPERSONIC AND HYPERSONIC FLOW OVER BLUNT BODIES. Division of Engineering, Brown University, WADC Tech. Note No. 57 - 349, 1957.
18. South, J. C., Jr. APPLICATION OF DORODNITSYN'S INTEGRAL METHOD TO NONEQUILIBRIUM FLOWS OVER POINTED BODIES. NASA TN D-1942, August 1963.
19. Traugott, S. C. AN APPROXIMATE SOLUTION OF THE DIRECT SUPERSONIC BLUNT-BODY PROBLEM FOR ARBITRARY AXISYMMETRIC SHAPES. Journal of Aerospace Sciences, Vol. 27, No. 5, pp. 361-370, May 1960.
20. Traugott, S. C. SOME FEATURES OF SUPERSONIC AND HYPERSONIC FLOW ABOUT BLUNTED CONES. Journal of Aerospace Sciences, Vol. 29, No. 4, pp. 389-399, April 1962.
21. Truitt, R. W. HYPERSONIC AERODYNAMICS. The Ronald Press Co., New York, 1959.

22. Uchida, S., and Yasuhara, M. THE ROTATIONAL FIELD BEHIND A CURVED SHOCK WAVE CALCULATED BY THE METHOD OF FLUX ANALYSIS. Journal of Aerospace Sciences, Vol. 23, No. 9, 1956.
23. Van Dyke, M. D. SUPERSONIC BLUNT-BODY PROBLEM -- REVIEW AND EXTENSION. Journal of Aerospace Sciences, Vol. 25, No. 8, pp. 485-497, August 1958.
24. Van Dyke, M. D., and Gordon, H. D. SUPERSONIC FLOW PAST A FAMILY OF BLUNT AXISYMMETRIC BODIES. NASA Rep. 1, 1959.

**The vita has been removed from
the scanned document**

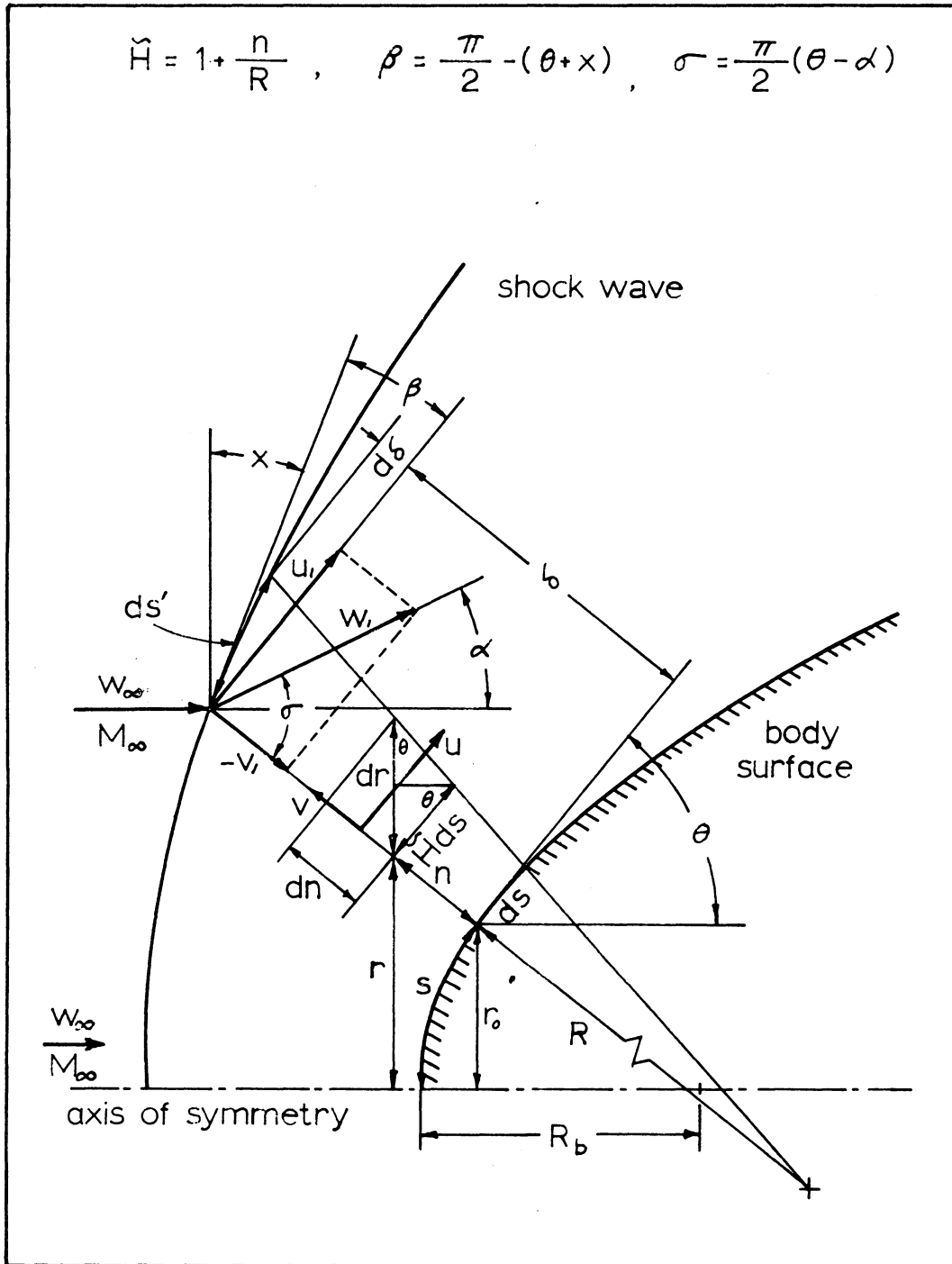


Fig. 1. Coordinate System and Associated Quantities

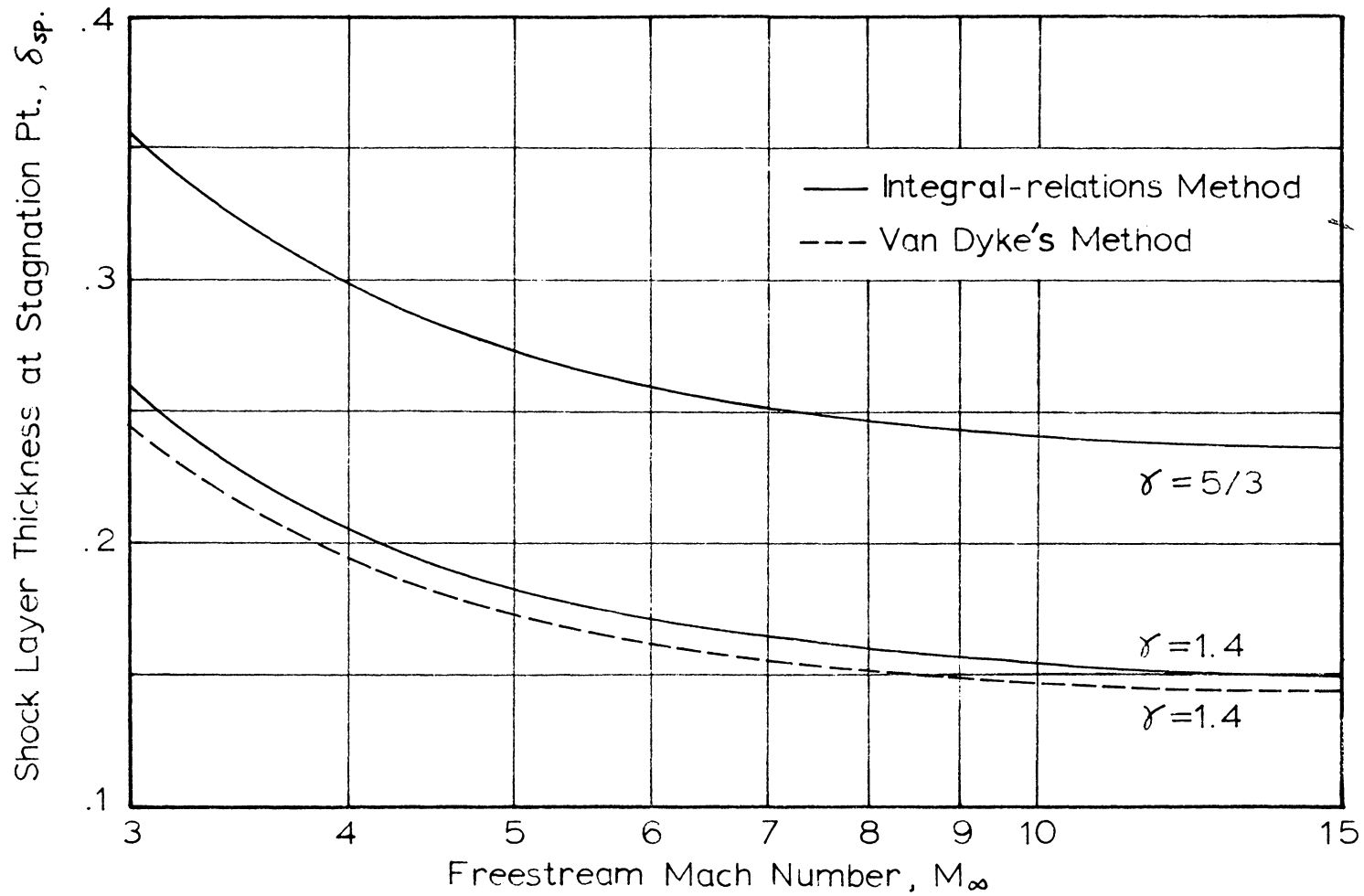


Fig. 2. Variation of Stagnation Shock Detachment Distance with Mach Number

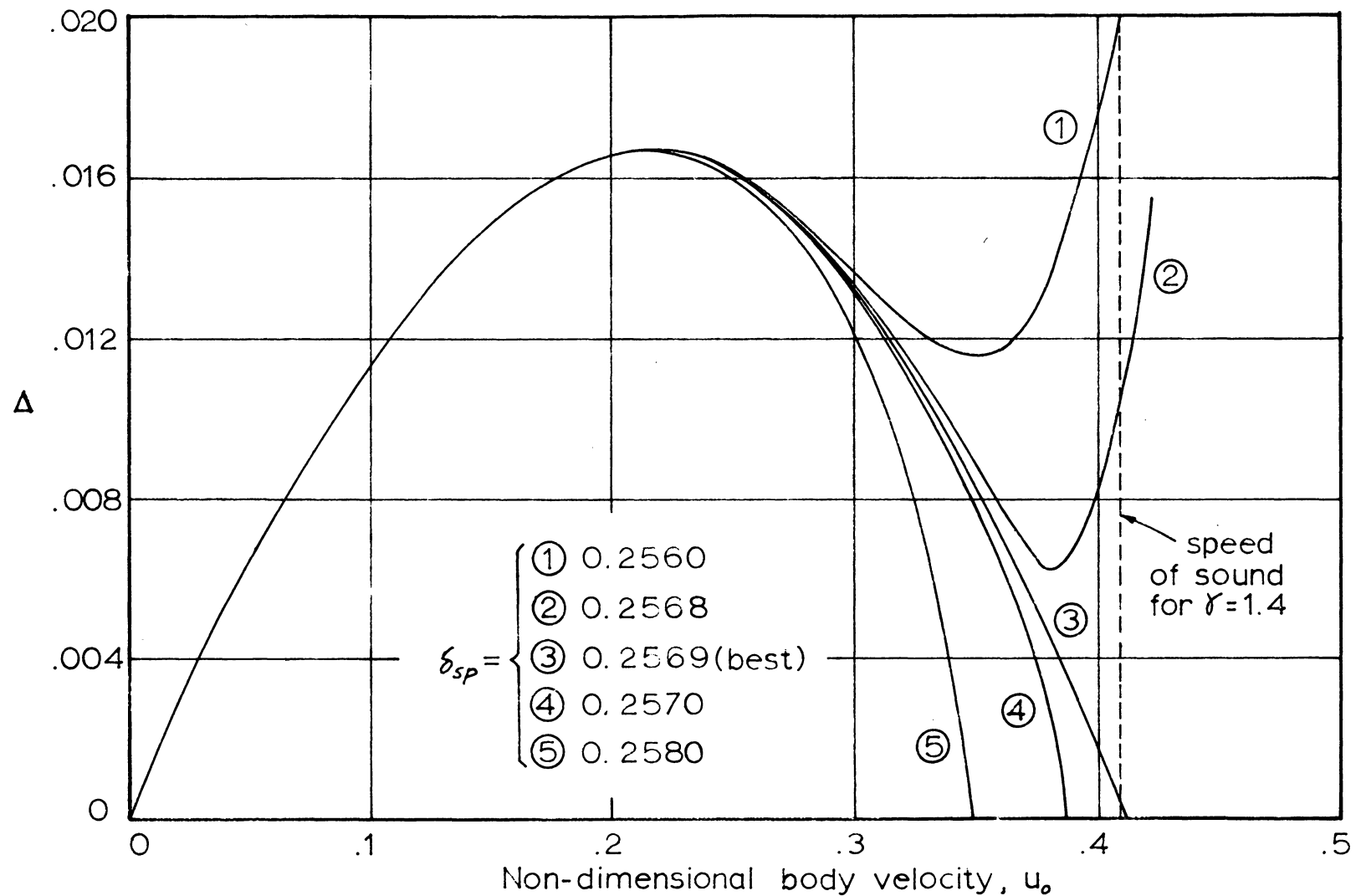


Fig. 3. Variation of Δ with u_0 for various δ_{sp} for $\gamma=1.4$ at $M_\infty=3$

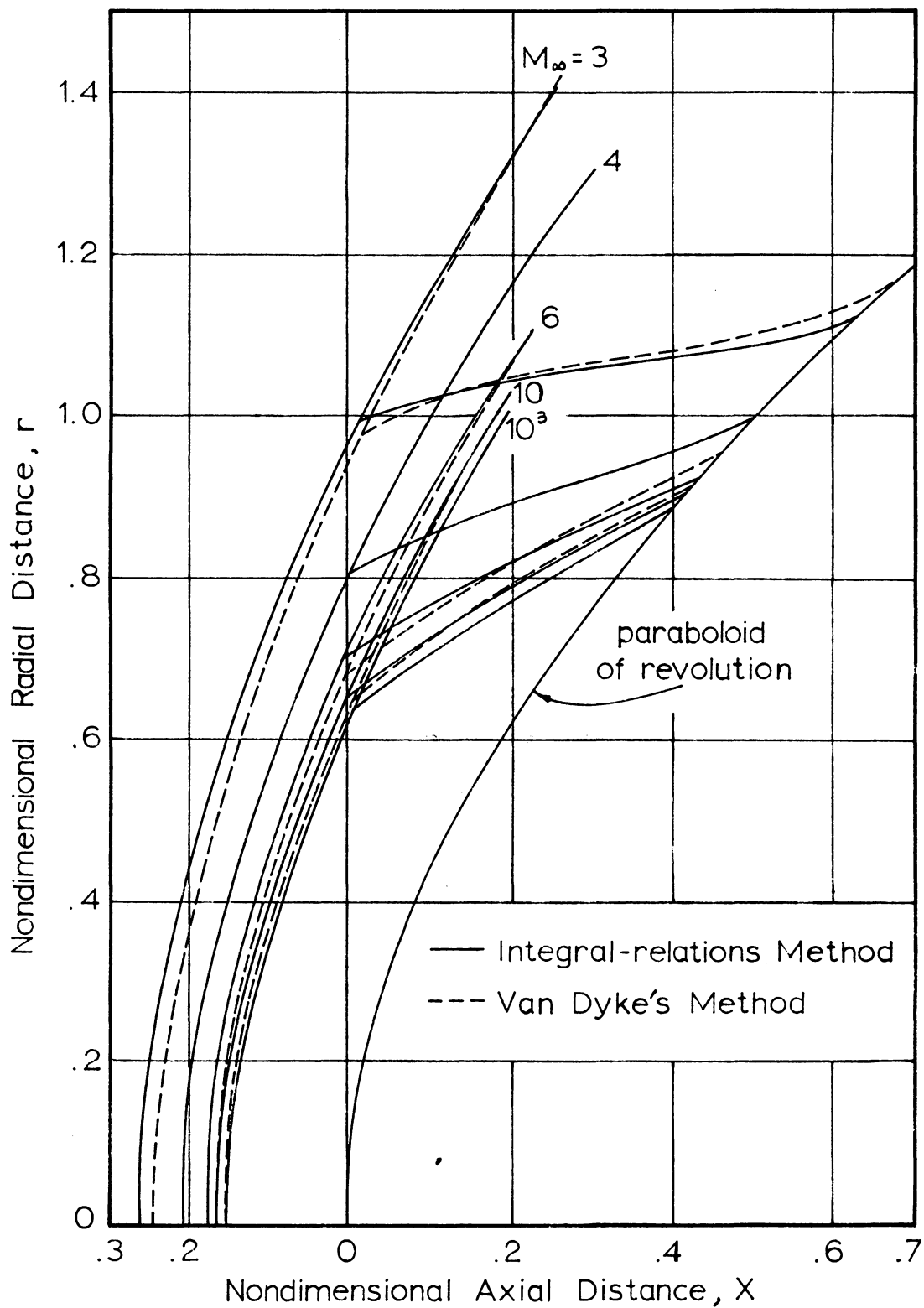


Fig. 4. Shock Shapes and Sonic Lines for $\gamma=1.4$

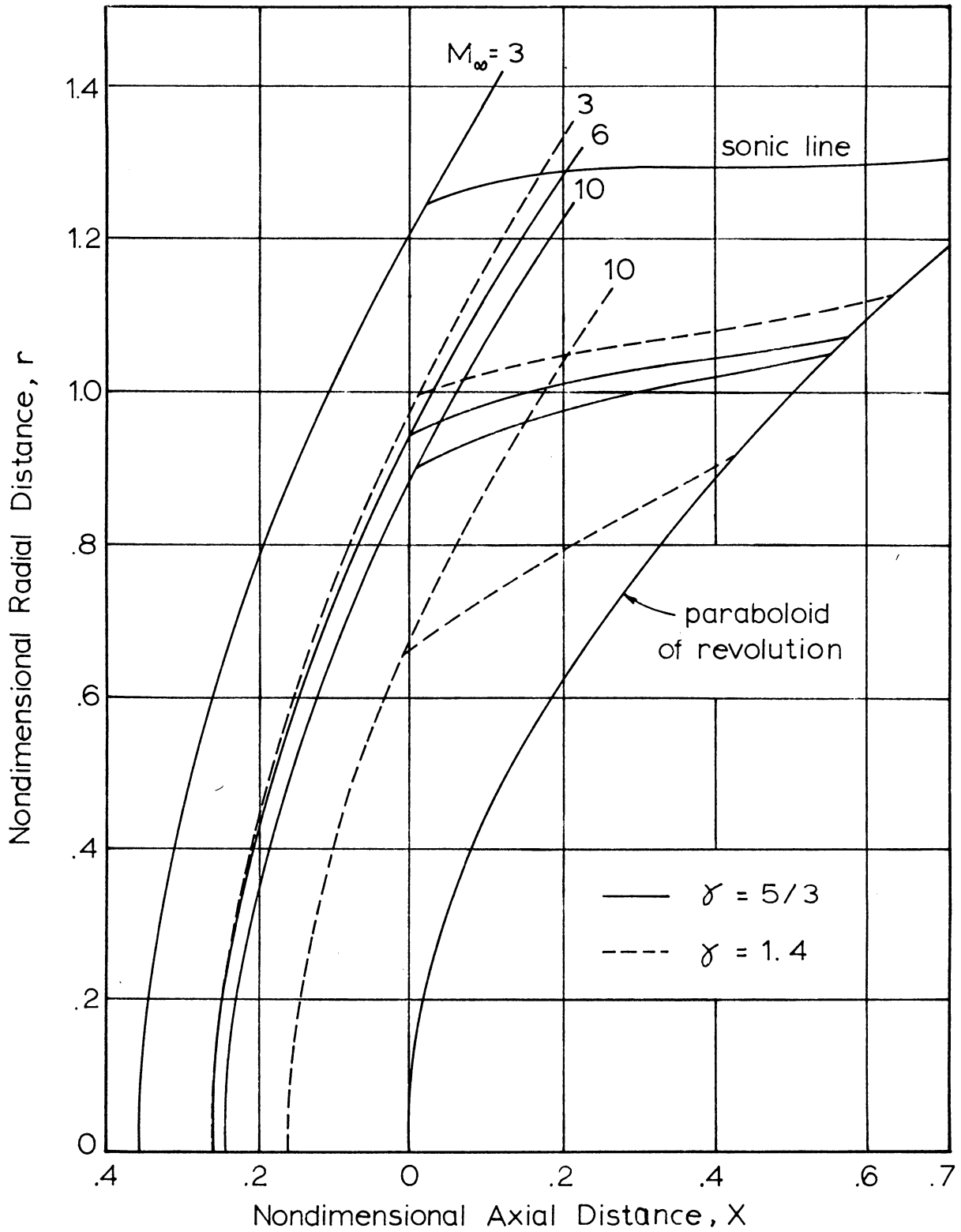


Fig. 5. Comparison of Shock Shapes for different γ

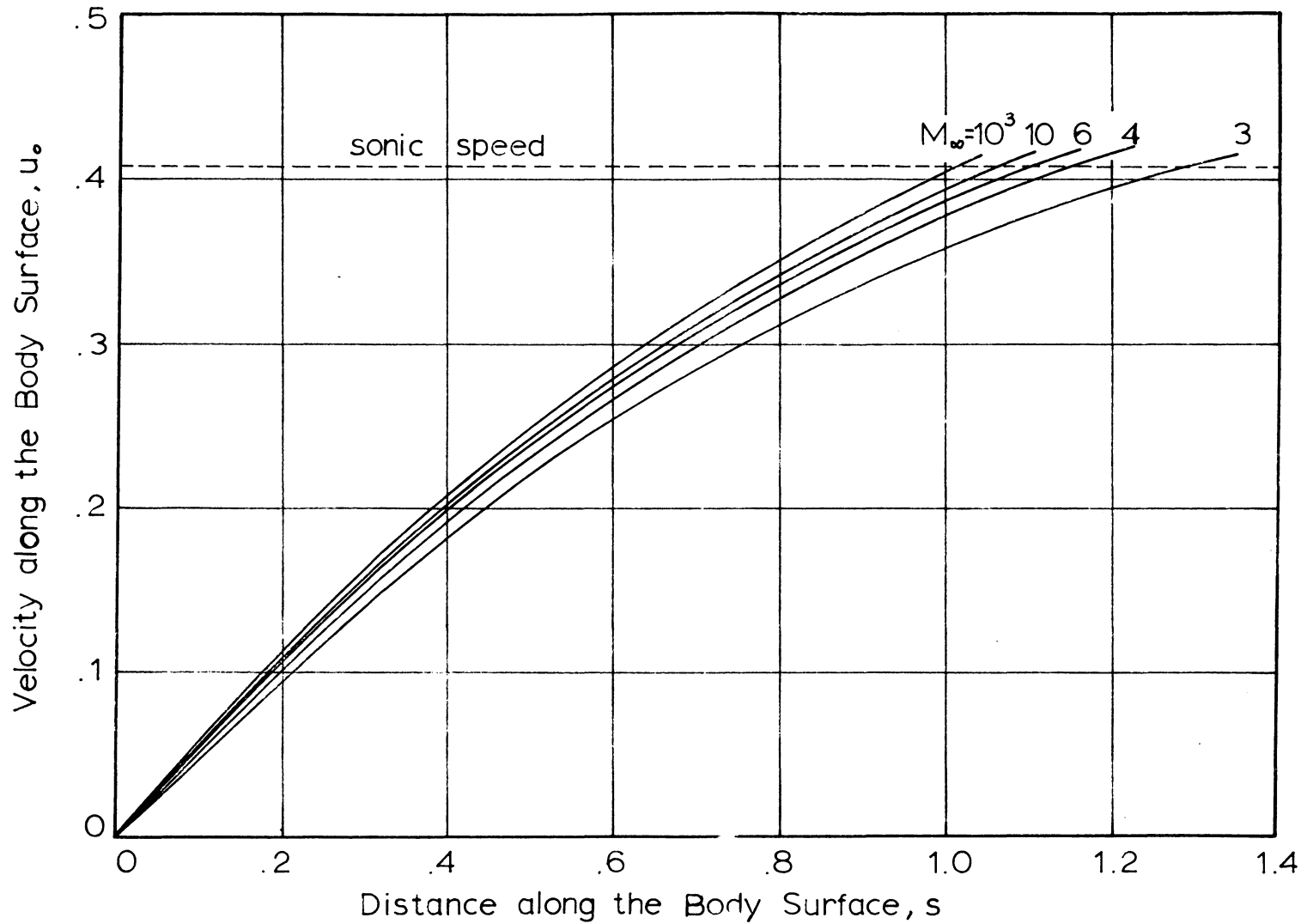


Fig. 6. Velocity Variation along the Body Surface for $\gamma=1.4$

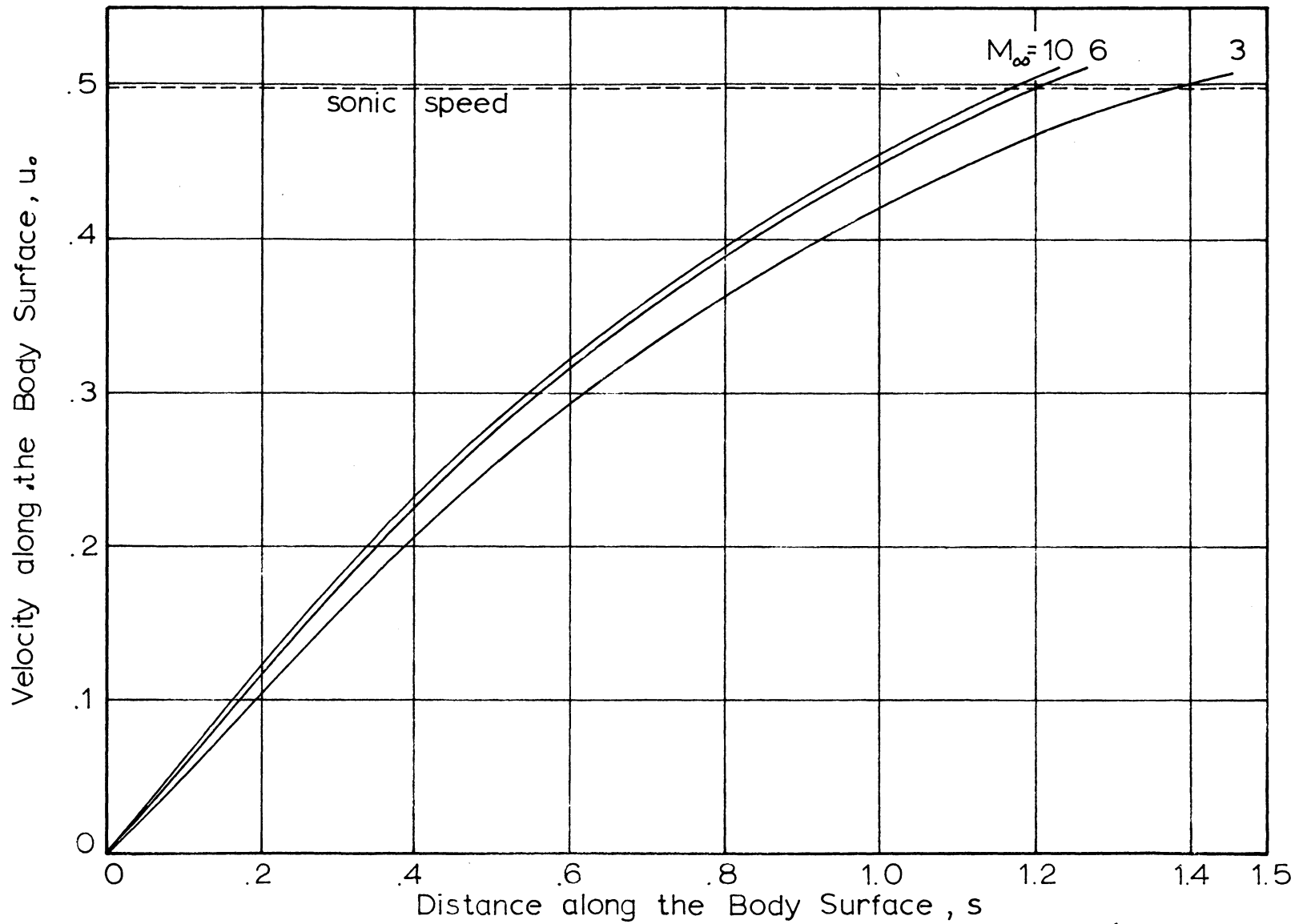


Fig. 7. Velocity Variation along the Body Surface for $\gamma = 5/3$

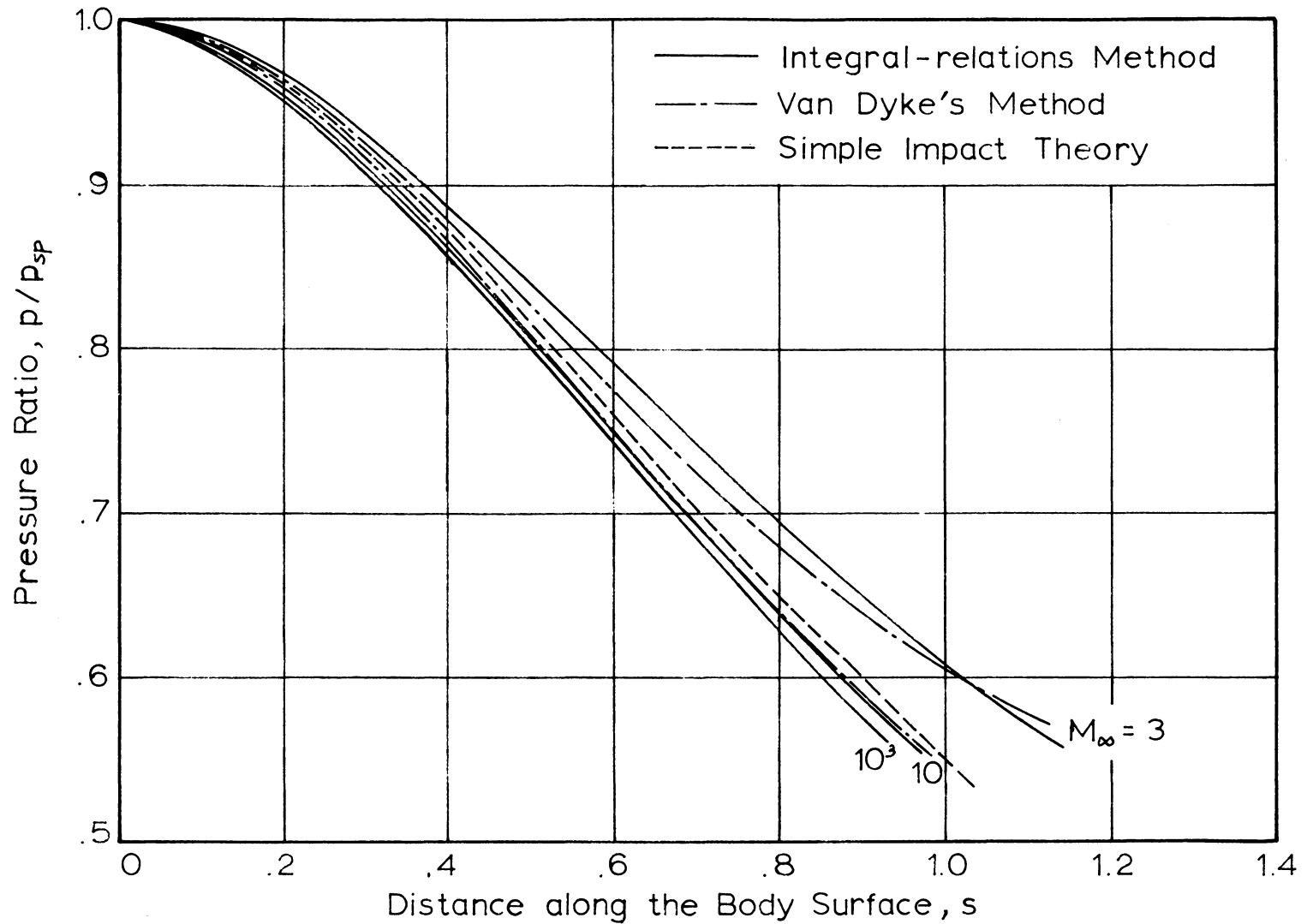


Fig. 8. Pressure Distribution on the Body Surface for $\gamma = 1.4$

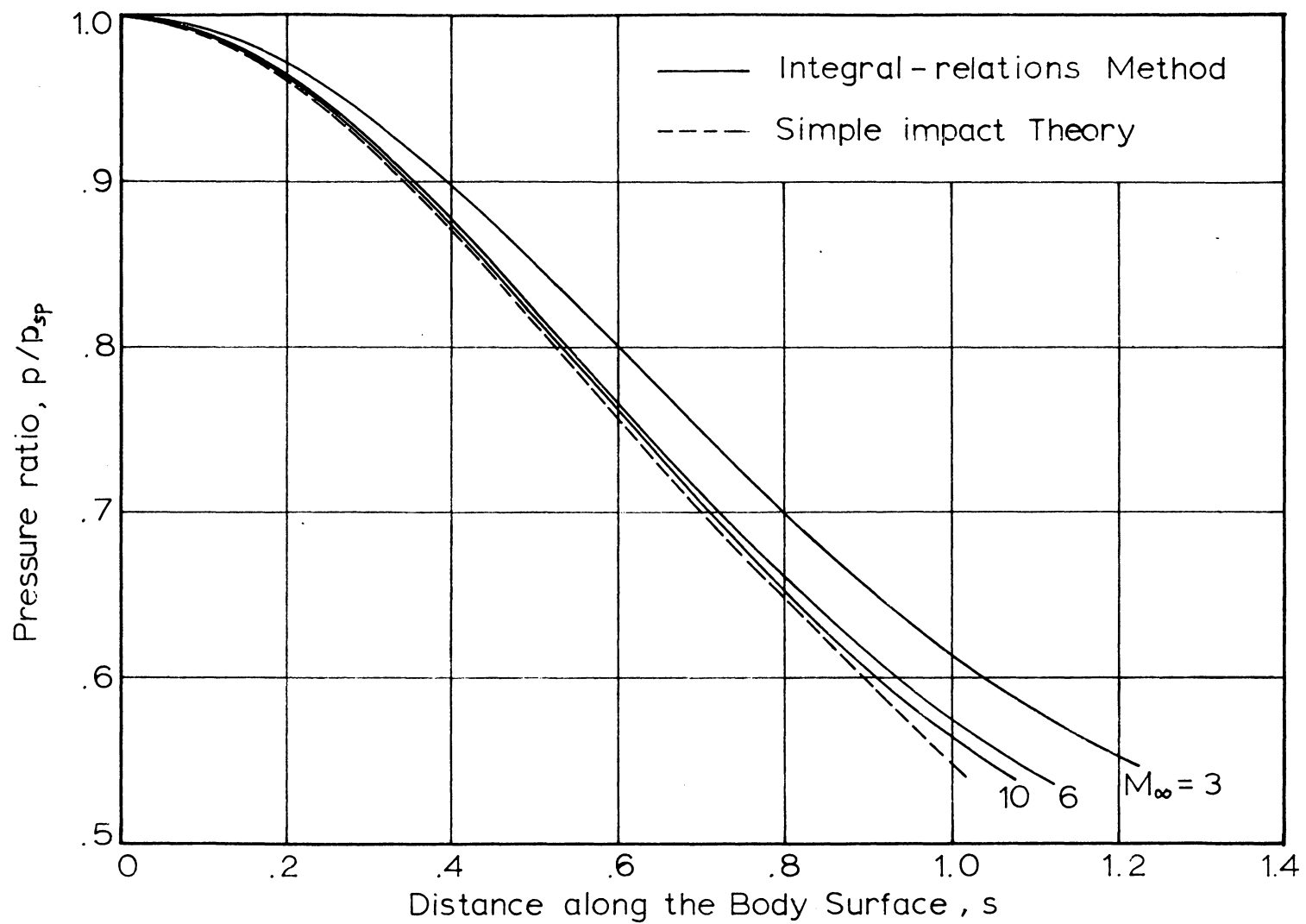


Fig. 9. Pressure Distribution on the Body Surface for $\gamma = 5/3$

APPLICATION OF THE METHOD OF INTEGRAL-RELATIONS
TO SUPERSONIC AND HYPERSONIC FLOW
PAST PARABOLOIDS OF REVOLUTION

by

Ming-Yang Su

ABSTRACT

Under the assumption of a perfect gas with a constant specific heat ratio, the first approximation of the integral-relations method, which considers the entire shock layer as a single strip, is derived for axisymmetric bodies of arbitrary smooth contour. The resulting differential equations were then applied to a supersonic and hypersonic flow past a paraboloid of revolution. The shock shapes, shock wave detachment distances, locations of sonic lines, and velocity and pressure distributions for the body were calculated for $\gamma = 1.4$ and $\gamma = 5/3$, and at Mach numbers of 3, 4, 6, 10 and 1000.

These calculations were carried out on an IBM 1620 electronic computer. The results were compared with those obtained by Van Dyke's inverse method. The agreement between the two methods was found to be good, in view of the fact that only the first approximation of the integral-relations method was used.